Hybrid density functional calculations of redox potentials and formation energies of transition metal compounds

V. L. Chevrier, S. P. Ong, R. Armiento, M. K. Y. Chan, and G. Ceder*
Department of Materials Science and Engineering, Massachusetts Institute of Technology, Cambridge, Massachusetts 02139, USA
(Received 12 February 2010; revised manuscript received 18 July 2010; published 12 August 2010)

We compare the accuracy of conventional semilocal density functional theory (DFT), the DFT+U method, and the Heyd-Scuseria-Ernzerhof (HSE06) hybrid functional for structural parameters, redox reaction energies, and formation energies of transition metal compounds. Conventional DFT functionals significantly underestimate redox potentials for these compounds. Zhou *et al.* [Phys. Rev. B **70**, 235121 (2004)] addressed this issue with DFT+U and a linear-response scheme for calculating U values. We show that the Li intercalation potentials of prominent Li-ion intercalation battery materials, such as the layered Li_xMO_2 (M=Co and Ni), Li_xTiS_2; olivine Li_xMPO_4 (M=Mn, Fe, Co, and Ni); and spinel-like $Li_xMn_2O_4$, $Li_xTi_2O_4$, are also well reproduced by HSE06, due to the self-interaction error correction from the partial inclusion of Hartree-Fock exchange. For formation energies, HSE06 performs well for transition metal compounds, which typically are not well reproduced by conventional DFT functionals but does not significantly improve the results of nontransition metal oxides. Hence, we find that hybrid functionals provide a good alternative to DFT+U for transition metal applications when the large extra computational effort is compensated by the benefits of (i) avoiding species-specific adjustable parameters and (ii) a more universal treatment of the self-interaction error that is not exclusive to specific atomic orbital projections on selected ions.

DOI: 10.1103/PhysRevB.82.075122 PACS number(s): 71.15.Mb, 71.15.Nc, 71.27.+a, 82.47.Aa

I. INTRODUCTION

Reduction and oxidation (redox) reactions are relevant in many technological applications and environmental processes, from electrochemical energy generation and storage systems such as fuel cells and rechargeable Li-ion batteries to corrosion processes. Owing to their importance, the development of first-principles techniques to study redox reactions has therefore been an area of considerable research interest.[1–5]

In redox reactions, electrons are transferred from one species to another. Previous work[3,4] has shown that the standard local-density (LDA) and generalized gradient approximation (GGA) to density functional theory (DFT) lead to considerable errors in calculated redox energies. These errors can be attributed in part to the lack of self-interaction error cancellation when the redox electron is transferred between significantly different environments, such as between metallic Li and an ionic transition metal (TM) environment in the case of Li intercalation compounds. Zhou *et al.*[3] demonstrated that treating the self-interaction error by means of the DFT+U method,[6–9] where the U parameter is determined by a linear-response scheme, leads to predicted Li intercalation potentials (also called voltages) for TM compounds that are in much better agreement with experiments. Wang *et al.*[4] found that the DFT+U method can similarly be applied to correct for self-interaction errors in the calculated reaction energies of TM oxides.

In this paper, we will revisit the calculation of Li intercalation potentials and formation energies of TM compounds, in the context of hybrid density functionals. The hybrid density functional modification of the DFT scheme has predominantly been used in molecular chemistry applications[10,11] but has more recently gained momentum in the solid-state community, possibly due to the introduction of hybrid functionals that are not specifically tailored for molecular chemistry applications.[12–15]

The exact Hartree-Fock (HF) exchange energy cancels the self-interaction error in the electron energy by construction.[16] It follows that the hybrid scheme of using a fraction of the HF exchange energy plus a fraction of a conventional semilocal functional cancels more of this error than using only the latter. Hybrid functionals, such as B3LYP, have also been found successful for calculations on simple TM oxides.[17–20] The improvement of the self-interaction error is expected to reduce the unwanted electron self-repulsion and thus, at least partially, avoid the well-known problem of overdelocalized electrons in LDA or GGA. Zhou *et al.*[3] argued that it was precisely such overdelocalization of d-orbital electrons on the TM ions that was responsible for the poor performance of conventional functionals for redox reactions, and this prompted their use of DFT+U. The argument thus motivates us to investigate the performance of hybrid functionals in the same type of applications. Our results are not only useful as a guide of the performance of hybrid functionals for calculations of TM compounds but also provide a set of uncomplicated examples where the self-interaction correction in the hybrid scheme correctly localizes electron states. This should be useful for understanding how and when hybrid functionals improves on conventional functionals. Finally, hybrid functionals, due to the lack of an adjustable U parameter, could provide for a more straightforward, though more expensive, prediction of redox energies.

The rest of the paper is organized as follows: in Sec. II, we discuss the methods used for calculating Li intercalation potentials and redox formation energies, and for selecting the compounds used in the different calculations, as well as details of the computational methods. In Sec. III, the calculated volumes, Li intercalation potentials, and formation energies for the selected compounds are presented. In Sec. IV, we

discuss the differences between the DFT, DFT+U, and hybrid calculations, specifically with the aim of understanding how the DFT+U and hybrid results differ in their treatment of the self-interaction error. Section V gives a summary and some concluding statements.

II. METHODS

A. Intercalation potentials of electrode materials

The average intercalation potential of Li into a host material vs Li/Li^+ is calculated using DFT.[21] The average intercalation potential, $\langle V \rangle$, when lithiating a material Li_xX from $x=x_1$ to x_2 is obtained from

$$\langle V \rangle = \frac{-[E(Li_{x_2}X) - E(Li_{x_1}X) - (x_2 - x_1)E(Li)]}{(x_2 - x_1)e}, \quad (1)$$

where E is the total energy as calculated using DFT, and e is the absolute value of the electron charge.

The materials studied in this paper were chosen to represent the major classes of intercalation materials currently used or under consideration as positive electrode materials in Li-ion batteries. The materials are briefly described and detailed descriptions can be found in the references indicated below. To calculate average Li intercalation potentials we considered complete, topotactic delithiation. Experimental lithiated structures were taken from the inorganic crystal structure database (ICSD) (Ref. 22) and delithiated structures were obtained by removing all Li atoms from the lithiated structures.

The traditional positive electrode materials are the $LiMO_2$ layered oxides (M=Co and Ni), which are favored for their high intercalation potentials and energy densities. The $LiMO_2$ layered oxides are O3-type structures, where the oxygen planes have an *ABCABC* stacking sequence.[23] In these structures, Li intercalates between layers of TM-centered oxygen octahedra. After complete delithiation, the MO_2 layers are weakly bound by van der Waals forces.[24] The layered oxides have been extensively studied both experimentally[25,26] and theoretically.[21,27–29]

Two Ti-containing materials were chosen in order to study materials having weakly localized 3d electrons. Li_xTiS_2 and $Li_xTi_2O_4$ both display metallic conductivities;[30,31] consequently, the delocalized Ti d states should not require the use of a U correction. The layered dichalcogenide, $LiTiS_2$ was once considered as a positive electrode material but its Li intercalation potential of 2.0 V was deemed too low to achieve reasonable energy densities.[30] Li_xTiS_2 is an O1-type layered structure, where the sulfur planes have an *ABAB* stacking sequence. Spinel $LiTi_2O_4$ also has a low Li intercalation potential (1.3 V) but can be used as a negative electrode in applications requiring excellent safety and power capability.[31] It is the only electrode material considered in this paper that does not undergo complete topotactic delithiation. In its lithiated state, $Li_2Ti_2O_4$, the Li atoms reside on the octahedral 16c sites of the $Fd3m$ (227) space group whereas in its delithiated state, $LiTi_2O_4$, the Li atoms reside on the tetrahedral 8a sites of the same space group.[32]

The spinel-like $LiMn_2O_4$ is popular for its high voltage (4.1 V) and reasonable cost.[25,33] It is isostructural with the spinel mineral $MgAl_2O_4$ and presents a three-dimensional network of face-sharing oxygen tetrahedra and octahedra. The Mn atoms reside in MnO_6 octahedra. In the lithiated structure, the Mn ions are evenly distributed in nominal Mn^{3+} and Mn^{4+} states.[34]

Finally, the olivine structures, $LiMPO_4$ (M=Mn, Fe, Co, and Ni) have received increased attention as positive electrode materials for large-scale applications.[35–38] The most commonly used olivine is $LiFePO_4$ due to its low cost, excellent safety, and reasonable potential (3.5 V).[35] The olivine structures are constituted of vertex-sharing MO_6 octahedra and PO_4 tetrahedra that share one edge and all vertices with MO_6 octahedra. The olivines are differentiated from the previously mentioned oxides, which will be referred to as "simple" oxides, by the presence of PO_4 polyanions. It is believed that the TM ions hybridize less with the PO_4 groups than with oxygen atoms of simple oxides.[39] The lack of hybridization should lead to a greater degree of localization of the 3d electrons on the TM ions and thereby increase the self-interaction error of LDA/GGA.

B. Oxide formation energies

Formation energies were calculated for 26 oxides for which experimental formation enthalpies are available.[40,41] The choice of oxides follows closely that of Ref. 4. The chosen oxides can be separated into two categories. The first category is comprised of oxides containing main group elements (Li, Na, Mg, Al, and Ca) and elements with weakly localized 3d electrons (Ti), while the second category consists of TMs with strongly localized 3d electrons (V, Cr, Mn, Fe, Co, Ni, and Cu). Following the methodology of Ref. 4, the formation energy, ΔH_O, for an oxide XO_x, was calculated per O_2 molecule,

$$\Delta H_O = \frac{2}{x}[E(XO_x) - E(X)] - E(O_2), \quad (2)$$

where $E(X)$ is the energy of X in its elemental state and $E(O_2)$ is the energy of an isolated O_2 molecule.

C. Computational methods

Spin-polarized total-energy calculations and structure relaxations were performed with the Vienna *ab initio* simulation package (VASP 5.2.2), using a 500 eV energy cutoff and appropriate k-point meshes to obtain a convergence of better than 10 meV/f.u. Structural relaxations were performed to a tolerance of 2×10^{-4} eV/atom in the total energy, yielding average forces of 0.01 eV/Å. TM atoms were initialized in high spin and low spin states, as well as in ferromagnetic (FM) and antiferromagnetic (AFM) orderings when relevant. The configuration yielding the lowest energy was kept as the ground state. All GGA calculations were performed with the Perdew-Burke-Ernzerhof (PBE) functional.[42] Projector-augmented wave[43] pseudopotentials included in the VASP distribution were used in all cases. In the case of Jahn-Teller active ions (Mn^{3+}, Ni^{3+}), Jahn-Teller distortions were allowed by explicitly breaking the symmetry of the cell. Primitive cells were used in all calculations except for $LiNiO_2$,

TABLE I. Values of the U parameters in electron volt, adapted from Ref. 3.

	Olivine	Layered	Spinel
Mn	4.5		4.8
Fe	4.3		
Co	5.7	5.1	
Ni	6.1	6.4	

where a cell of 6 f.u. was used to allow Jahn-Teller distortions.

Rotationally invariant,[8] spherically averaged[9] GGA+U calculations were performed, where only a single effective interaction parameter, U, is required to characterize the localization of the 3d electrons. Table I lists the U values used for the calculation of intercalation potentials. These values were obtained by averaging the U values found in Ref. 3 over the redox states found in the lithiated/delithiated structures. The U values in Ref. 3 were obtained using a linear-response scheme.

Hybrid calculations were performed using the HSE06 functional[13–15] as implemented in VASP. The HSE06 functional starts from the PBE0 functional,[12] which is an implementation of the Becke three-parameter hybrid formula[11,44] that combines PBE exchange E_x^{PBE} and correlation E_c^{PBE} with HF exchange E_x^{HF},

$$E_{xc}^{\mathrm{PBE0}} = \frac{1}{4}E_x^{\mathrm{HF}} + \frac{3}{4}E_x^{\mathrm{PBE}} + E_c^{\mathrm{PBE}}. \quad (3)$$

In HSE06, the exchange terms are divided into short-range and long-range parts, and to avoid the expensive calculation of long-range HF exchange, this term is replaced by long-range PBE exchange,

$$E_{xc}^{\mathrm{HSE}} = \frac{1}{4}E_x^{\mathrm{HF,SR}}(\mu) + \frac{3}{4}E_x^{\mathrm{PBE,SR}}(\mu) + E_x^{\mathrm{PBE,LR}}(\mu) + E_c^{\mathrm{PBE}}, \quad (4)$$

where the screening parameter μ=0.207 Å^{-1} was determined as a compromise between speed and accuracy from a test set of molecules and solids.[13] The screening approach of HSE06 produces a hybrid functional that has a similar accuracy to PBE0 but is less computationally demanding.

III. RESULTS

A. Geometries and electronic structures

Table II shows the volumes obtained with GGA, GGA+U, and HSE06 after full relaxation of atomic positions and cell parameters. Experimental volumes are listed when available. Figure 1 shows the relative error compared to experiment.

The volumes for the lithiated layered oxides ($LiCoO_2$, $LiNiO_2$) obtained with HSE06 are underestimated by 1.5% on average while the volumes obtained with GGA and GGA+U are overestimated by 1.6% on average. The difference in volume between functionals is not isotropic across cell parameters. Table III shows the cell parameters obtained for $LiCoO_2$. In the layered structures, the a parameter is determined by M-O bond lengths within the layers, while the c parameter denotes layer separation. HSE06 is known to generally predict shorter and more accurate bond lengths than GGA and GGA+U,[13,14] and indeed predicts the most accurate cell parameters. GGA predicts a larger a parameter but a smaller c parameter than HSE06. The same relation for the lattice parameters is also found for the other layered materials, $LiNiO_2$ and $LiTiS_2$. These differences may be related to the different types of bonding present in the structures. Li^+ ions are found between M-O layers, indicating the layers are

TABLE II. Volume per formula unit obtained after complete structural optimization with GGA, GGA+U, and HSE06 compared to experiment. Lithiated formula units are listed in the structure column, and delithiation corresponds to complete topotactic removal of Li atoms. GGA+U values in parenthesis indicate the use of GGA values (equivalent to U=0), and are included to make mean errors comparable. The mean absolute relative error (MARE) in percentage is indicated and calculated when experimental phases are available.

	Delithiated Volume (Å/f.u.)					Lithiated Volume (Å/f.u.)				
Structure	GGA	GGA+U	HSE06	Expt.	Ref.	GGA	GGA+U	HSE06	Expt.	Ref.
$LiCoO_2$	33	34	32	29.61	24	33.00	32.86	31.81	32.17	45
$LiNiO_2$	33	33	33	30.86	46	34.58	34.16	33.41	34.07	47
$LiTiS_2$	65	(65)	62	57.32	48	63.95	(63.95)	64.92	64.12	48
$Li_2Ti_2O_4$ [a]	75.72	(75.72)	75.50	74.18	32	73.65	(73.65)	74.35	73.44	32
$LiMn_2O_4$	66.93	70.74	65.81	66.36	33	67.84	73.88	70.25	69.89	49
$LiMnPO_4$	72.95	73.59	70.93	68.67	36	77.11	77.97	75.70	75.50	36
$LiFePO_4$	72.57	71.76	70.00	68.09	39	74.39	75.10	72.92	72.85	39
$LiCoPO_4$	71.62	68.01	66.08	69.67	37	72.31	73.28	71.22	70.98	37
$LiNiPO_4$	64.18	69.33	67.06			70.54	70.55	68.76	68.62	50
MARE (%)	6.5	7.3	4.5			1.7	2.3	0.8		

[a]Delithiation to $LiTi_2O_4$.

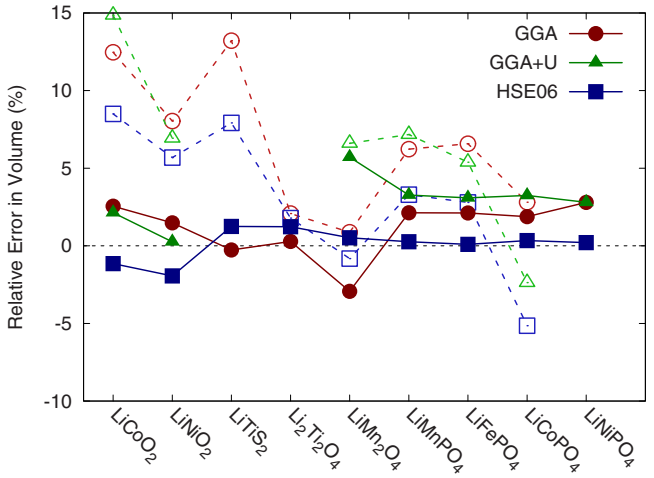

FIG. 1. (Color online) Relative error of the optimized volumes compared to experiment for the lithiated phases when using GGA, GGA+U, and HSE06. Lighter, open symbols indicate corresponding delithiated phases, with complete topotactic delithiation for all phases except to $LiTi_2O_4$ for $Li_2Ti_2O_4$. References for experimental volumes are found in Table II.

bound to each other through ionic-type interactions (in the c direction) while M-O bonds though ionic in nature, have significantly more hybridization and characterize the a parameter.

$LiNiO_2$ contains Ni^{3+} Jahn-Teller ions, and similar Jahn-Teller distortions were found in GGA+U and HSE06 calculations. The four short and two long Ni-O bonds being 1.90 Å and 2.14 Å, respectively, for GGA+U, and 1.88 Å and 2.13 Å, respectively, for HSE06. These results are in reasonable agreement with the experimental values of 1.91 Å and 2.07 Å.[51]

The delithiated layered materials (CoO_2, NiO_2, and TiS_2) have a much larger error in volume than their lithiated counterparts, with mean absolute relative errors of 10% and 1.3%, respectively. A very shallow potential was found for their interlayer spacing with GGA, GGA+U, and HSE06. Indeed, variations in only a few millielectron volt per formula unit per angstrom in interlayer spacing (parallel to the c axis) were observed. The volumes are therefore quoted to fewer significant figures in Table II. The interaction between layers in delithiated layered materials is mainly of a van der Waals type and therefore is not accurately modeled using GGA, GGA+U, or HSE06. For all three delithiated layered materials, the calculated volumes are larger than experimental values, reflecting the lack of van der Waals interactions in these methods.

TABLE III. Cell parameters for $LiCoO_2$, space group $R\bar{3}m$ (166).

	a (Å)	c (Å)
GGA	2.856	14.009
GGA+U	2.832	14.193
HSE06	2.804	14.018
Expt. (Ref. 45)	2.816	14.054

The lithiated Ti-containing structures ($LiTiS_2$, $Li_2Ti_2O_4$) have smaller volumes with GGA than with HSE06, where GGA is closer to experiment. The smaller GGA volumes correlate with smaller magnetic moments; the magnetic moments of the Ti atoms obtained with GGA were 0.58 and 0.01 μ_B, and with HSE06 0.86 and 0.95 μ_B for $LiTiS_2$ and $Li_2Ti_2O_4$, respectively.

$LiMn_2O_4$ is the only structure where GGA significantly underestimates the volume compared to experiment. Low-temperature AFM $LiMn_2O_4$ spinel is experimentally known to have charge disproportionation,[34] with distributed Mn^{3+} and Mn^{4+} ions. Comparison of the magnetic moments of the four Mn ions in the primitive cell of $LiMn_2O_4$ reveals that GGA is unable to achieve charge disproportionation, and yields Mn ions with an identical average valence. GGA+U and HSE06 both succeed in yielding charge disproportionation, evidenced by two pairs of Mn ions in the primitive cell with different magnetic moments corresponding to Mn^{3+} and Mn^{4+} both in high spin states. The Mn^{3+} ions are Jahn-Teller active and the experimental values for the short and long bond lengths are 1.94 Å and 2.29 Å, respectively.[52] Jahn-Teller distortions were only found in MnO_6 octahedra centered on Mn^{3+} ions in GGA+U and HSE06 calculations. The distortions were characterized by short and long bond lengths of 1.97 Å and 2.21 Å, respectively, for GGA+U and 1.94 Å and 2.19 Å, respectively, for HSE06, in reasonable agreement with experiment. The lack of charge disproportionation and Jahn-Teller distortions in GGA are likely the cause of the lower volume obtained with GGA when compared to experiment.

The lithiated olivine structures yield a consistent ordering of volumes as a function of calculation method. The volumes obtained with GGA, GGA+U, and HSE06 are on average 2%, 3%, and 0.2% greater than experiment, respectively. The error and variability compared to experiment is greater for the delithiated phases. The volumes obtained for the olivines with GGA and GGA+U are in good agreement with previously reported values.[3] All the lithiated and delithiated olivine structures were found to be AFM with the exception of $LiCoPO_4$ (GGA+U, HSE06) and $NiPO_4$ (GGA, GGA+U, HSE06), which were found to be FM. High spin states of the expected valence where always found on the TM ions, with the exception of $NiPO_4$. The magnetic moments obtained with HSE06 were slightly smaller than those obtained with GGA+U for all the lithiated and delithiated olivine structures except $NiPO_4$. The magnetic moment of the Ni ion in $NiPO_4$ was unexpectedly low with GGA+U and was *greater* by 0.3 μ_B with HSE06. Previous spin-polarized LDA calculations have found the olivine structures to be semimetals[53] while spin-polarized GGA+U calculations have found them to be insulators.[54] The HSE06 functional yields insulators for all lithiated and delithiated olivine materials.

The $MnPO_4$ olivine structure contains high spin Mn^{3+} ions that are Jahn-Teller active. Jahn-Teller distortions were obtained with all calculation methods with two pairs of short and one pair of long Mn-O bonds: 1.88, 1.97, and 2.43 Å (GGA); 1.91, 2.00, and 2.40 Å (GGA+U); and 1.86, 1.96, and 2.40 Å (HSE06).

TABLE IV. Average Li intercalation potentials vs. Li/Li^+ in volts, obtained using GGA, GGA+U, and HSE06 for complete delithiation compared to experiment. Parentheses indicate the use of the GGA value (U=0). Experimental potentials have an estimated error of ±0.1 V.

	GGA	GGA+U	HSE06	Expt.	Ref.
$LiCoO_2$	3.38	3.85	4.51	4.1	24
$LiNiO_2$	3.08	3.92	4.14	3.9	26
$LiTiS_2$	1.91	(1.91)	2.06	2.1	30
$Li_2Ti_2O_4$ [a]	1.05	(1.05)	1.19	1.3	31
$LiMn_2O_4$	3.37	4.04	4.25	4.1	33
$LiMnPO_4$	2.99	4.01	3.87	4.1	36
$LiFePO_4$	2.84	3.47	3.33	3.5	35
$LiCoPO_4$	3.62	4.63	4.57	4.8	37
$LiNiPO_4$	4.15	5.00	5.41	5.3[b]	38
Mean	2.93	3.54	3.70	3.69	
MAE[c]	0.76	0.15	0.19		

[a]Delithiation to $LiTi_2O_4$.
[b]$LiNiPO_4$ is unstable upon delithiation, leading to a larger error in average intercalation potential.
[c]Mean absolute error.

Finally, general trends can be established when comparing geometries obtained with GGA, GGA+U, and HSE06. Figure 1 shows that the lithiated volumes are generally more accurate than delithiated volumes for all calculation methods. Table II lists the mean absolute relative errors compared to experiment. HSE06 is consistently in better agreement with experiment with a mean absolute relative error of only 0.8%. These results are consistent with previous findings indicating that hybrid methods correct the typical GGA underbinding.[55] The volumes obtained with GGA+U yield the greatest mean absolute relative error for both the lithiated and delithiated structures. Although not shown, the magnetic moments of the TM ions obtained with HSE06 were on average less than those obtained with GGA+U by only 0.08 μ_B and greater than those obtained with GGA by 0.3 μ_B.

The selection of oxide compounds for the study of formation energies follows that of Ref. 4. Full optimizations of atomic positions and cell parameters were performed for all structures. Calculations were performed using GGA and HSE06. The AFM or FM orderings obtained are identical to those found in Ref. 4. The magnetic moments obtained with GGA are within numerical uncertainties of those obtained in Ref. 4. The magnetic moments obtained with HSE06 were on average 0.05 μ_B per TM atom smaller than the magnetic moments obtained with GGA+U in Ref. 4. Geometry optimizations for the oxides with GGA and HSE06 yielded mean absolute relative errors of 2.6% and 1.6% in volume, respectively, compared to experiment.

Total energies of pure elemental solids are required for the calculation of formation energies. Optimizations of the elemental structures with GGA and HSE06 yielded mean absolute relative errors of 3.6% and 5.9% in volume, respectively, compared to experiment. These results are consistent with the literature indicating hybrid methods are least successful in systems that are governed by delocalized electrons, such as elemental metals.[14] Elemental Cr and Mn were outliers from the elemental HSE06 mean absolute relative error. For Cr the AFM ordering of Ref. 56 yielded the lowest energy structure with a HSE06 volume 23% greater than experiment. Elemental Mn has a very complex magnetic structure. Calculations were initialized with the collinear AFM ordering of Ref. 57 yielding a HSE06 volume 18% greater than experiment. Details of the Mn magnetic structure can be found in the supplementary materials.[58]

The space groups for all the positive electrode and binary oxide materials can be found in the supplementary materials.[58] The supplementary materials also include the lowest energy magnetic structure, the average of the magnetic moments, and the band gap derived from the electronic density of states (DOS) for all the structures.

B. Intercalation potentials

Lithium intercalation potentials are obtained using Eq. (1). Table IV lists the Li intercalation potentials obtained with GGA, GGA+U, and HSE06 while Fig. 2 shows the intercalation potential errors with respect to experiment.

For the layered oxides, HSE06 yields potentials that are significantly overestimated. As previously published,[3,21] GGA severely underestimates the potentials by 0.7 V on average while GGA+U with a linear response U yields values close to experiment.

The Ti-containing structures ($LiTiS_2$, $Li_2Ti_2O_4$) do not require the use of a U correction because of the absence of localized 3d electrons in Ti. This is confirmed by the agreement with experiment of the GGA Li intercalation potentials for these structures. The agreement with experiment of the GGA intercalation potentials is significantly better for the Ti-containing compounds than for any of the other TM-containing compounds. The potentials obtained with HSE06 are greater than those obtained with GGA by 0.15 V and are in better agreement with experiment.

The Li intercalation potentials obtained for $LiMn_2O_4$ with HSE06 and GGA+U are both nearly within experimental

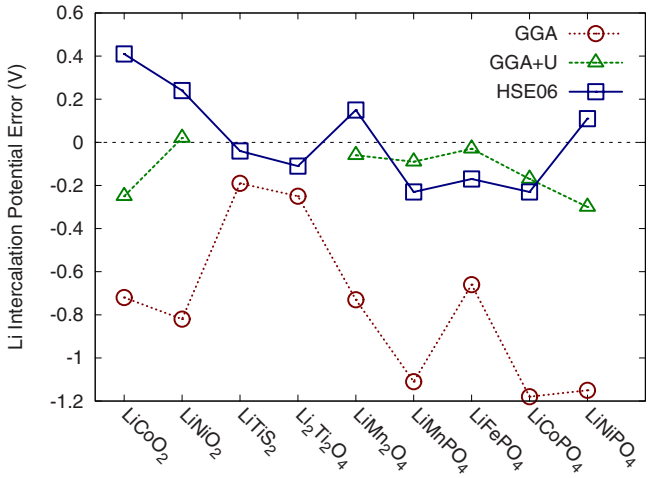

FIG. 2. (Color online) Difference between calculated and experimental Li intercalation potentials for GGA, GGA+U, and HSE06.

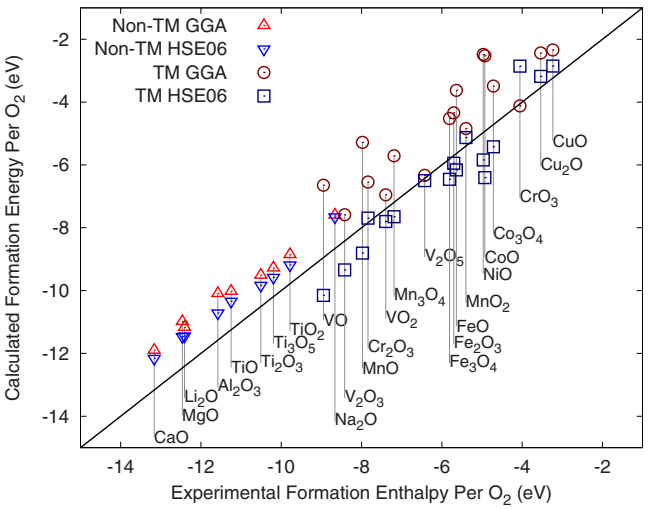

FIG. 3. (Color online) Formation energies of oxides per O_2 calculated with GGA and HSE06 plotted against experimental formation enthalpies (Refs. 40 and 41).

error. The HSE06 potential is greater than the one obtained with GGA+U by 0.21 V. Once more, GGA underestimates the potential by approximately 0.7 V.

The olivines (LiMPO$_4$, M=Mn, Fe, Co, and Ni) yield potentials which are underestimated on average by 1 V with GGA. The Mn, Fe, and Co olivines are the only materials where the Li intercalation potentials obtained with HSE06 are smaller than those obtained with GGA+U and by experiment. The smaller Li intercalation potentials obtained with HSE06 are correlated with the presence of the PO_4 polyanion. As opposed to the other olivines, the Li intercalation potential obtained for $LiNiPO_4$ with HSE06 is greater than those obtained with GGA+U and by experiment. As previously stated, $NiPO_4$ was also the only olivine structure where the Ni magnetic moments obtained with HSE06 were greater than those obtained with GGA+U.

C. Oxide formation energies

The O_2 molecule has an experimental binding energy of −5.12 eV.[40] GGA is known to overbind for O_2, and a value of −6.04 eV was obtained with GGA in good agreement with previous calculations.[4,59] HSE06 yields a binding energy of −5.16 eV, in much better agreement with experiment than GGA. According to the methodology of Ref. 4, one would therefore not expect HSE06 to introduce significant O_2 binding errors in the calculation of formation energies for nontransition metal oxides, where there is little correlation error on the metal ion.

Figure 3 shows the formation energy of various oxides when starting from their elemental form as calculated with GGA and HSE06, compared to experiment.[40,41] The GGA formation energies are consistent with those of Ref. 4.

The GGA formation energy of the oxides of metals without localized 3d electrons (Li, Na, Mg, Al, Ca, and Ti) is underestimated by a nearly constant error of 1.18 eV compared to experiment (the exclusion of Ti-containing oxides yields an average error of 1.32 eV, in agreement with Ref. 4). The TM oxides containing atoms with localized 3d electrons (V, Cr, Mn, Fe, Co, Ni, and Cu) have much more scatter in their calculated GGA formation energies and have an average error of 1.32 eV (σ=0.20 eV).

The HSE06 nontransition metal oxide formation energies are very similar to those obtained with GGA, although the average error is slightly less at 0.85 eV. The TM oxides with HSE06 yield formation energies that have less scatter than with GGA and have an average error of −0.35 eV (σ =0.15 eV). The agreement with experiment of formation energies for TM oxides is therefore better with HSE06 than with GGA.

IV. DISCUSSION

A. Electrode materials

Table II and Fig. 1 indicate that HSE06 presents a significant gain in accuracy over GGA+U and GGA for structural parameters of lithiated and delithiated compounds without the need for adjustable parameters. The HSE06 functional should therefore have better predictive capabilities for volumes and volume changes upon lithiation. While the volumetric capacity (charge/volume) of an electrode material is an important characteristic, the error obtained with GGA or GGA+U is well behaved and not large enough to be relevant to materials screening.

Jahn-Teller distortions have important, practical consequences for electrode materials.[25,60–63] Mechanical degradation can occur upon cycling if the lithiation or delithiation of an electrode changes the valence state of a TM atom from a Jahn-Teller active to an inactive state. The anisotropic structural changes caused by Jahn-Teller distortions have been claimed to contribute to electrode failure in $LiNiO_2$, $Li_2Mn_2O_4$, and $LiMnPO_4$.[25,60,61] GGA, GGA+U, and HSE06 all yield similar Jahn-Teller distortions in systems without charge disproportionation. In the presence of charge disproportionation, such as $LiMn_2O_4$, only GGA+U and HSE06 successfully yield Jahn-Teller distortions. HSE06 is therefore

capable of yielding charge disproportionation, one of the key advantages of GGA+U over GGA in the study of electrode materials.

For all the positive electrode materials, the ground-state magnetic ordering was the same in both GGA+U and HSE06. The magnetic moments obtained with HSE06 were on average slightly lower than those obtained with GGA +U, indicating that HSE06 leads to less localization of the 3d electrons. However, the localization of the 3d electrons in GGA+U depends on the U parameter. In this study, the U values were taken from a linear-response approach but other methods can be used to determine U,[64–67] such as fitting to experimental reaction energies.[4]

One of the most important properties of an electrode material in Li-ion batteries is the Li intercalation potential. The intercalation potential difference between the negative and positive electrode dictates the energy associated with every lithiation/delithiation and must be within a range that is compatible with the electrolyte of the Li-ion cell. HSE06 is much more successful than GGA in predicting intercalation potentials in the presence of localized electrons with a mean absolute error of 0.2 V compared to 0.9 V with GGA. In the absence of localized electrons, such as in Ti oxides or sulfides, HSE06 and GGA yield similar intercalation potentials. GGA+U with a linear-response U successfully reproduces experimental intercalation potentials with a mean absolute error of 0.1 V for TM-containing electrode materials with localized d electrons. The *average error* is therefore smaller for GGA+U than HSE06 though it is not clear whether this difference in accuracy between GGA+U and HSE06 is statistically significant given our small data set. In GGA+U a correction to the self-interaction energy is only applied to the projected d states of the TM atoms. However, in HSE06 the use of HF exchange leads to corrections of self-interaction errors directly on all occupied eigenstates. The HSE06 functional should correct self-interaction errors in oxygen atoms as well, and the bonding environment of the oxygen atoms may therefore have a greater impact on redox energies in HSE06 than in GGA+U. This indeed appears to be the case as HSE06 yields higher intercalation potentials than GGA +U for simple oxides ($LiCoO_2$, $LiNiO_2$, and $LiMn_2O_4$) but lower intercalation potentials for the polyanion-containing olivines ($LiMPO_4$, M=Mn, Fe, and Co).

Figure 4 shows the difference in charge densities obtained with HSE06 and GGA+U ($\rho^{\mathrm{HSE06}}-\rho^{\mathrm{GGA+U}}$) for the layered oxides at an isosurface level of ± 0.02 $e/\text{Å}^3$. GGA+U calculations were performed with HSE06 geometries in order to obtain comparable charge densities. The yellow (lighter) and blue (darker) isosurfaces indicate where HSE06, respectively, locates more or less charge than GGA+U. It is clear that GGA+U locates more charge on the TM atom, while HSE06 locates more charge on the oxygen atom in both the lithiated and delithiated layered oxides, indicating that HSE06 tolerates hybridization between the oxygen p and TM d orbitals more than GGA+U, which forces localization in the TM d orbitals. The effect appears to be more pronounced for Li_xCoO_2 than for Li_xNiO_2 as the isosurface volumes of Li_xCoO_2 are larger, which may be a reflection of more delocalized states and of the metallic nature of Li_xCoO_2.[69] Figures 2 and 4, respectively, show a higher intercalation potential and greater localization of charge on the oxygen atoms with HSE06 for Li_xCoO_2 than for Li_xNiO_2. Indeed, the intercalation potential obtained with HSE06 for $LiCoO_2$ is 0.7 V greater than with GGA+U, compared to 0.22 V for $LiNiO_2$. The Li intercalation potential depends on the energy difference between the lithiated and delithiated structures. One may speculate that the correction of self-interaction errors with HSE06 in the simple oxides stabilizes charge localization on the oxygen, thereby stabilizing the lithiated state and consequently raising the intercalation potential.

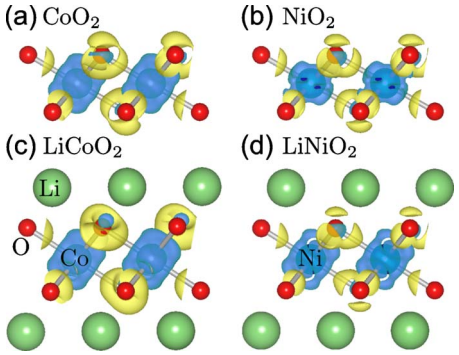

FIG. 4. (Color online) Isosurface of the difference between charge densities obtained with HSE06 and GGA+U ($\rho^{\mathrm{HSE06}}-\rho^{\mathrm{GGA+U}}$). The yellow (lighter) and blue (darker) represent the positive and negative 0.02 $e/\text{Å}^3$ isosurfaces, respectively. View along [01$\bar{1}$], rendered using VESTA (Ref. 68).

As opposed to the simple oxides, for the $LiMPO_4$ (M =Mn, Fe, and Co) olivines HSE06 underestimates the Li intercalation potentials compared to GGA+U and experiment. Figure 5 shows the difference in charge densities obtained with HSE06 and GGA+U ($\rho^{\mathrm{HSE06}}-\rho^{\mathrm{GGA+U}}$) for MPO_4 and $LiMPO_4$ (M=Fe and Ni) at an isosurface of ± 0.02 $e/\text{Å}^3$. Figure 5(a) shows that in $FePO_4$ GGA+U localizes slightly more charge on the Fe and P ions than HSE06, and less around the oxygen atom along the Fe-O and P-O bonds. Figure 5(c) shows that in $LiFePO_4$ GGA+U once again localizes more charge on the Fe ion than HSE06. Com-

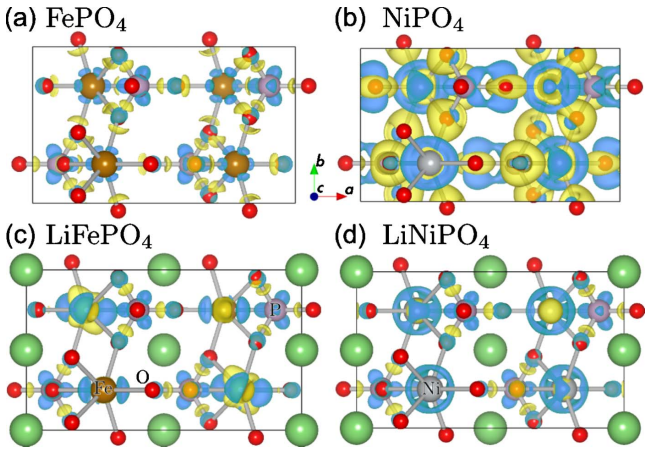

FIG. 5. (Color online) Isosurface of the difference between charge densities obtained with HSE06 and GGA+U ($\rho^{\mathrm{HSE06}}-\rho^{\mathrm{GGA+U}}$). The yellow (lighter) and blue (darker) represent the positive and negative 0.02 $e/\text{Å}^3$ isosurfaces, respectively.

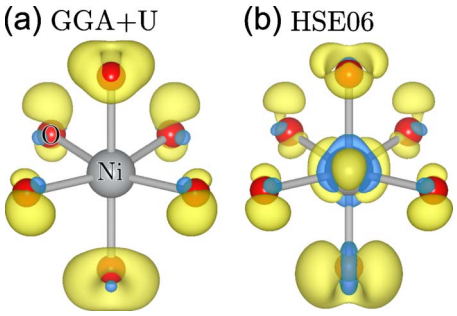

FIG. 6. (Color online) Isosurfaces of the change in charge density upon lithiation of $NiPO_4$ to $LiNiPO_4$ ($\rho_{LiNiPO_4}-\rho_{NiPO_4}$) with (a) GGA+$U$ and (b) HSE06. The yellow and blue represent the positive and negative 0.054 $e/Å^3$ isosurfaces, respectively. Only the NiO_6 octahedra is shown as no difference was visible on the P atom at the chosen isosurface value.

parison of Figs. 5(a) and 5(c) shows that differences in charge densities between HSE06 and GGA+U in the PO_4 polyanion are practically unchanged upon lithiation from $FePO_4$ to $LiFePO_4$. The ($\rho^{HSE06}-\rho^{GGA+U}$) charge-density differences obtained for the simple oxides in Fig. 4 are greater than the charge-density differences obtained for Li_xFePO_4 in Figs. 5(a) and 5(c). Indeed the greater charge localization on the oxygen obtained with HSE06 compared to GGA+U is more pronounced in the simple oxides than in the olivines. This is likely the cause of the lower HSE06 intercalation potentials for the olivines compared to GGA+U and the higher HSE06 intercalation potentials for the simple oxides compared to GGA+U. The strong covalent bonding in the PO_4 group leads to less M-O hybridization. The decreased M-O hybridization in the olivines leads to less charge transfer to the oxygen upon lithiation than in the simple oxides. Hence, the correction of the self-interaction errors on oxygen orbitals by HSE06 may therefore have less of an impact in the olivines, and stabilization of the lithiated state by HSE06 may therefore not be as pronounced with the olivines than with the simple oxides, leading to lower intercalation potentials compared to GGA+U.

The Li intercalation potential obtained for $LiNiPO_4$ is higher with HSE06 than with GGA+U. Li_xNiPO_4 therefore behaves differently than the other olivines, which yield higher intercalation potentials with GGA+U. Figures 5(b) and 5(d) show the difference in charge densities obtained with HSE06 and GGA+U for $NiPO_4$ and $LiNiPO_4$. Figures 5(c) and 5(d) are very similar, showing $LiFePO_4$ and $LiNiPO_4$ have very similar differences in charge densities, however a comparison of Figs. 5(a) and 5(b) shows a marked contrast between the differences in charge densities for $FePO_4$ and $NiPO_4$. Figure 5(b) shows HSE06 and GGA+U yield electronic structures for $NiPO_4$ that are much more different than for the other olivines.

Charge transfer in electrode materials can be studied by subtracting the charge densities of lithiated and delithiated structures.[21] This was done for $LiNiPO_4/NiPO_4$ with HSE06 and GGA+U. Figure 6 shows the ± 0.054 $e/Å^3$ isosurfaces for the charge-density differences: ($\rho^{HSE06}_{LiNiPO_4}-\rho^{HSE06}_{NiPO_4}$), and ($\rho^{GGA+U}_{LiNiPO_4}-\rho^{GGA+U}_{NiPO_4}$). Figure 6(a) shows there is no charge transfer occurring on the Ni ion with GGA+U upon lithiation of $NiPO_4$ at this isosurface level. The absence of charge transfer on the Ni atom indicates the Ni atom is in the same valence state in both $NiPO_4$ and $LiNiPO_4$ with GGA+U. Based on the magnetic moment of the Ni ion, it appears Ni is found in a Ni^{2+} state in both $NiPO_4$ and $LiNiPO_4$ with GGA+U. Figure 6(b) shows the Ni ion gains charge upon lithiation with HSE06, furthermore the positive isosurface shape is characteristic of a t_{2g} orbital, which is consistent with a Ni^{3+} to Ni^{2+} reduction with both ions in a high spin state.

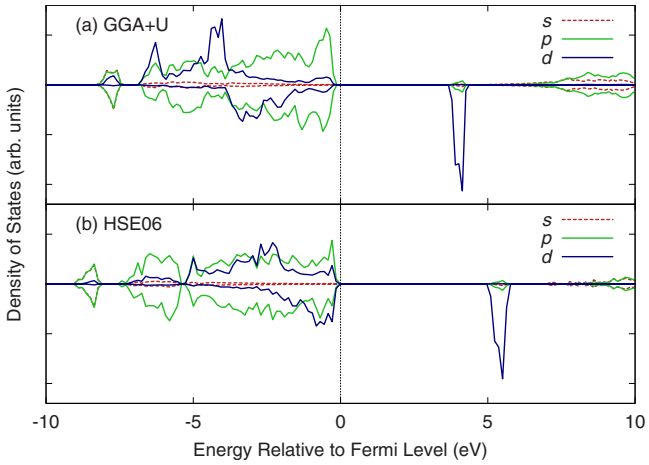

FIG. 7. (Color online) Summed projected DOS of atoms having parallel magnetic moments in AFM $LiNiPO_4$ calculated using (a) GGA+U and (b) HSE06.

Based on the observed charge transfer upon Li insertion, we can argue that in GGA+U the relative position of the Ni and oxygen electronic levels near the Fermi level in Li_xNiPO_4 is different than in HSE06, we can further confirm this by examining the projected DOS. Figure 7 shows the summed projected DOS of the atoms in $LiNiPO_4$ having parallel magnetic moments. Since the ground-state magnetic ordering of $LiNiPO_4$ is AFM, excluding the contributions to the projected DOS of the atoms having antiparallel magnetic moments allows the identification of the spin features in the DOS. Figure 7 shows the oxygen levels are higher in energy than the Ni levels with GGA+U while oxygen and Ni levels are found at similar energies and have greater hybridization with HSE06. Observations of a similar nature have previously been reported for NiO. Indeed, the relative position of Ni and oxygen levels in NiO have been investigated both experimentally[70,71] and theoretically.[72] When a Ni^{2+} is replaced by a Li^+ in a NiO crystal, the resulting hole is seen to reside on the oxygen. The removal of Li from $LiNiPO_4$ can be seen as the addition of a hole. GGA+U places the hole on the oxygen while HSE06 distributes the hole over both Ni and O. The presence of a PO_4 polyanion makes Li_xNiPO_4 significantly different from NiO, and it is not obvious which result more accurately represents reality. Agreement with the experimental Li intercalation potential may not be the best metric since the intercalation potential of Li_xNiPO_4 is very high and above the potential of standard electrolytes. Furthermore, only a single account of electrochemical cycling of $LiNiPO_4$ was found in the literature and the intercalation potential was determined from only one cycle.[38] Assuming

HSE06 yields a more accurate description of the physics occurring in Li_xNiPO_4, one may speculate GGA+U is in fact underestimating the Li intercalation potential of Li_xNiPO_4.

B. Oxides

The formation of oxides requires the transfer of electrons between significantly different environments. Wang *et al.*[4] have shown that oxide formation energies obtained with GGA have errors stemming from two main causes. The first is the overbinding of the O_2 molecule. The second is the lack of correction for self-interaction errors found in correlated states such as TM 3*d* orbitals.

The overbinding of the O_2 molecule in GGA can be addressed by artificially using a corrected value for the O_2 energy. Highly correlated electrons can be addressed by using GGA+U in the oxides. However, GGA+U with the same U cannot be used for TMs in their elemental forms as correct metallic states will not be obtained. GGA+U can therefore only be used for reaction energies involving solely oxides.

HSE06 yields an accurate bonding energy for the O_2 molecule, and largely corrects self-interaction errors in localized electronic states. One would therefore expect HSE06 to give significantly more accurate oxide formation energies than GGA. Figure 3 shows that HSE06 does indeed produce slightly more accurate formation energies for the nontransition metal oxides, as well as more accurate and less scattered formation energies for the TM oxides. However, it is surprising to realize that after correcting the nontransition metal oxide formation energies for the binding error in the O_2 molecule, the GGA results are actually closer to experiment than HSE06. After correction, the average errors compared to experiment are 0.26 eV and 0.81 eV for GGA and HSE06, respectively. For the TM oxides, after correcting for the O_2 binding energy, HSE06 is only slightly more accurate than GGA.

C. Benefits and drawbacks of hybrids compared to GGA+U

The greatest drawback of hybrid methods compared to GGA+U is computational cost. While the screening introduced in HSE06 makes it less costly than its unscreened limit, PBE0,[73] computational cost with HSE06 was still on average 40× greater than with GGA+U for the calculations reported in this paper. The intercalation potential of $LiNiO_2$ was calculated with PBE0 to verify that the screening introduced in HSE06 did not significantly affect the values of calculated intercalation potentials. The intercalation potential obtained with PBE0 was only 20 mV greater than the one obtained with HSE06. The PBE0 and HSE06 calculations were performed with identical *k*-point grids and therefore the PBE0 result is not as well converged as the HSE06 result. Indeed, the screening of HSE06 facilitates the energy convergence with respect to *k* points.[55]

The greatest advantage of HSE06 over GGA+U is that it is a parameter free, structure-agnostic functional. In GGA+U, the U parameter is species and environment dependent. It is therefore up to the user to determine if the U parameter is appropriate for a given species in a given structure and calculations with different U parameters cannot directly be used together, giving GGA+U calculations with a specific value of U limited span in composition space. This is not the case with HSE06, as it does not contain any species- or environment-dependent parameters. However, HSE06 does contain fixed parameters that could be varied: the HF mixing ($\frac{1}{4}$) and screening (μ) of Eq. (4).

The physical results obtained with GGA+U and HSE06 in this paper are nearly equivalent for Jahn-Teller distortions, charge disproportionation, magnetic moments, and magnetic ordering. HSE06 yields more accurate volumes while GGA+U with a linear response U yields slightly more accurate Li intercalation potentials. HSE06 and GGA+U yielded significantly different physics only in the case of Li_xNiPO_4, which has an extremely high intercalation potential. The choice between HSE06 and GGA+U will therefore depend on the resources available. For simple intercalation potential calculations, if a U parameter is available, HSE06 does not present major advantages which outweigh its greater cost. However, HSE06 may be required to study specific questions which benefit from the correction of self-interaction errors for all occupied eigenstates as opposed to only the ones treated with a U parameter. In addition, HSE06 is a consistent approach that can be used across all oxidation states, whereas the U parameter in GGA+U would change with valence state and would not be applicable to the metallic state.

V. SUMMARY AND CONCLUSION

Redox reactions are important in many technological and environmental processes. DFT calculations using GGA functionals fail to model these reactions when they involve localized electrons, such as the 3*d* electrons of TMs. The applicability of screened hybrid methods to the study of redox reactions in the presence or absence of localized electrons has been demonstrated.

The screened hybrid functional HSE06 was compared to GGA and GGA+U for the study of electrode materials and oxide formation. The correction of self-interaction errors in HSE06 through the use of HF exchange leads to a more accurate treatment of the 3*d* electrons in TM atoms. HSE06 is as successful as GGA+U in predicting Jahn-Teller distortions, magnetic moments, and charge localization. HSE06 consistently predicts more accurate geometries than both GGA and GGA+U. HSE06 and GGA+U with a linear response U yield similar accuracies for Li intercalation potentials. However, HSE06 does not require any adjustable parameters and is applicable irrespective of the type of atoms present in the structures of interest.

The prediction of Li intercalation potentials with HSE06 is sensitive to the bonding environment of the oxygen, in a way not found in GGA+U. The correction of self-interaction errors for all eigenstates with HSE06 appears to lead to greater charge localization on the oxygen orbitals in the simple oxides. The correction of self-interaction errors stemming from the oxygen atoms may stabilize charge transfer to the oxygen and be the cause of the higher intercalation potentials obtained with HSE06 for the simple oxides. The presence of PO_4 polyanions appears to mitigate this effect,

leading to lower intercalation potentials with HSE06.

HSE06 yields more accurate oxide formation energies than uncorrected GGA. GGA+U cannot be used for the calculation of oxide formation energies involving TMs because the same U cannot be used to properly model the metallic states of TMs in their elemental form.

The computational cost is greater for HSE06 than for GGA or GGA+U. For the study of redox reactions involving localized electrons, the choice between HSE06 and GGA+U will therefore hinge on the availability of an appropriate U, whether metallic states need to be modeled, and the available computational resources.

ACKNOWLEDGMENTS

This work was supported by the U.S. Department of Energy under Contract No. DE-FG02-96ER45571 and the Massachusetts Institute of Technology's Center for Materials Science and Engineering under Grant No. DMR-819762. Additional computing resources were provided through the Teragrid under Grant No. TG-DMR970008S.

*gceder@mit.edu

[1] K. S. Raymond, A. K. Grafton, and R. A. Wheeler, J. Phys. Chem. B **101**, 623 (1997).
[2] M. Uudsemaa and T. Tamm, J. Phys. Chem. A **107**, 9997 (2003).
[3] F. Zhou, M. Cococcioni, C. A. Marianetti, D. Morgan, and G. Ceder, Phys. Rev. B **70**, 235121 (2004).
[4] L. Wang, T. Maxisch, and G. Ceder, Phys. Rev. B **73**, 195107 (2006).
[5] C. J. Cramer and D. G. Truhlar, Phys. Chem. Chem. Phys. **11**, 10757 (2009).
[6] V. I. Anisimov, J. Zaanen, and O. K. Andersen, Phys. Rev. B **44**, 943 (1991).
[7] V. I. Anisimov, I. V. Solovyev, M. A. Korotin, M. T. Czyżyk, and G. A. Sawatzky, Phys. Rev. B **48**, 16929 (1993).
[8] A. I. Liechtenstein, V. I. Anisimov, and J. Zaanen, Phys. Rev. B **52**, R5467 (1995).
[9] S. L. Dudarev, G. A. Botton, S. Y. Savrasov, C. J. Humphreys, and A. P. Sutton, Phys. Rev. B **57**, 1505 (1998).
[10] A. D. Becke, J. Chem. Phys. **98**, 1372 (1993).
[11] A. D. Becke, J. Chem. Phys. **98**, 5648 (1993).
[12] C. Adamo and V. Barone, J. Chem. Phys. **110**, 6158 (1999).
[13] J. Heyd, G. E. Scuseria, and M. Ernzerhof, J. Chem. Phys. **118**, 8207 (2003).
[14] J. Paier, M. Marsman, K. Hummer, G. Kresse, I. C. Gerber, and J. G. Angyan, J. Chem. Phys. **125**, 249901 (2006).
[15] J. Heyd, G. E. Scuseria, and M. Ernzerhof, J. Chem. Phys. **124**, 219906 (2006).
[16] R. M. Martin, *Electronic Structure* (Cambridge University Press, New York, 2004).
[17] F. Corà, M. Alfredsson, G. Mallia, D. S. Middlemiss, W. C. Mackrodt, R. Dovesi, and R. Orlando, Struct. Bonding (Berlin) **113**, 171 (2004).
[18] X.-B. Feng and N. M. Harrison, Phys. Rev. B **69**, 035114 (2004).
[19] M. Alfredsson, G. D. Price, C. R. A. Catlow, S. C. Parker, R. Orlando, and J. P. Brodholt, Phys. Rev. B **70**, 165111 (2004).
[20] F. Tran, P. Blaha, K. Schwarz, and P. Novák, Phys. Rev. B **74**, 155108 (2006).
[21] M. K. Aydinol, A. F. Kohan, G. Ceder, K. Cho, and J. D. Joannopoulos, Phys. Rev. B **56**, 1354 (1997).
[22] A. Belsky, M. Hellenbrandt, V. L. Karen, and P. Luksch, Acta Crystallogr., Sect. B: Struct. Sci. **58**, 364 (2002).
[23] C. Delmas, C. Fouassier, and P. Hagenmuller, Physica B & C **99**, 81 (1980).
[24] G. G. Amatucci, J.-M. Tarascon, and L. C. Klein, J. Electrochem. Soc. **143**, 1114 (1996).
[25] M. M. Thackeray, J. Electrochem. Soc. **142**, 2558 (1995).
[26] C. Delmas, M. Menetrier, L. Croguennec, S. Levasseur, J. P. Peres, C. Pouillerie, G. Prado, L. Fournes, and F. Weill, Int. J. Inorg. Mater. **1**, 11 (1999).
[27] C. Wolverton and A. Zunger, J. Electrochem. Soc. **145**, 2424 (1998).
[28] J. Reed, G. Ceder, and A. Van der Ven, Electrochem. Solid-State Lett. **4**, A78 (2001).
[29] A. Van der Ven and G. Ceder, Electrochem. Solid-State Lett. **3**, 301 (2000).
[30] M. S. Whittingham, Science **192**, 1126 (1976).
[31] K. M. Colbow, J. R. Dahn, and R. R. Haering, J. Power Sources **26**, 397 (1989).
[32] R. J. Cava, D. W. Murphy, S. M. Zahurak, A. Santoro, and R. S. Roth, J. Solid State Chem. **53**, 64 (1984).
[33] M. A. Monge, J. M. Amarilla, E. Gutierrez-Puebla, J. A. Campa, and I. Rasines, ChemPhysChem **3**, 367 (2002).
[34] J. Rodríguez-Carvajal, G. Rousse, C. Masquelier, and M. Hervieu, Phys. Rev. Lett. **81**, 4660 (1998).
[35] A. Yamada, S. C. Chung, and K. Hinokuma, J. Electrochem. Soc. **148**, A224 (2001).
[36] G. H. Li, H. Azuma, and M. Tohda, Electrochem. Solid-State Lett. **5**, A135 (2002).
[37] K. Amine, H. Yasuda, and M. Yamachi, Electrochem. Solid-State Lett. **3**, 178 (2000).
[38] J. Wolfenstine and J. Allen, J. Power Sources **142**, 389 (2005).
[39] A. K. Padhi, K. S. Nanjundaswamy, and J. B. Goodenough, J. Electrochem. Soc. **144**, 1188 (1997).
[40] M. W. Chase, *NIST-JANAF Thermochemical Tables* (American Chemical Society, New York, 1998).
[41] O. Kubaschewski, C. B. Alcock, and P. I. Spencer, *Materials Thermochemistry* (Pergamon Press, Oxford, 1993).
[42] J. P. Perdew, K. Burke, and M. Ernzerhof, Phys. Rev. Lett. **77**, 3865 (1996).
[43] P. E. Blöchl, Phys. Rev. B **50**, 17953 (1994).
[44] J. P. Perdew, M. Emzerhof, and K. Burke, J. Chem. Phys. **105**, 9982 (1996).
[45] J. Akimoto, Y. Gotoh, and Y. Oosawa, J. Solid State Chem. **141**, 298 (1998).
[46] W. Li, J. N. Reimers, and J. R. Dahn, Solid State Ionics **67**, 123 (1993).
[47] A. Hirano, R. Kanno, Y. Kawamoto, Y. Takeda, K. Yamaura,

M. Takano, K. Ohyama, M. Ohashi, and Y. Yamaguchi, Solid State Ionics **78**, 123 (1995).
[48] J. R. Dahn, W. R. McKinnon, R. R. Haering, W. J. L. Buyers, and B. M. Powell, Can. J. Phys. **58**, 207 (1980).
[49] K. S. Yoo, N. W. Cho, and Y.-J. Oh, Solid State Ionics **113-115**, 43 (1998).
[50] O. García-Moreno, M. Alvarez-Vega, F. García-Alvarado, J. García-Jaca, J. M. Gallardo-Amores, M. L. Sanjuán, and U. Amador, Chem. Mater. **13**, 1570 (2001).
[51] C. Delmas, J. P. Peres, A. Rougier, A. Demourgues, F. Weill, A. Chadwick, M. Broussely, F. Perton, P. Biensan, and P. Willmann, J. Power Sources **68**, 120 (1997).
[52] R. Hoppe, G. Brachtel, and M. Jansen, Z. Anorg. Allg. Chem. **417**, 1 (1975).
[53] Y.-N. Xu, W. Y. Ching, and Y.-M. Chiang, J. Appl. Phys. **95**, 6583 (2004).
[54] F. Zhou, K. Kang, T. Maxisch, G. Ceder, and D. Morgan, Solid State Commun. **132**, 181 (2004).
[55] J. Paier, M. Marsman, K. Hummer, G. Kresse, I. C. Gerber, and J. G. Angyan, J. Chem. Phys. **124**, 154709 (2006).
[56] J. Kübler, J. Magn. Magn. Mater. **20**, 277 (1980).
[57] D. Hobbs, J. Hafner, and D. Spišák, Phys. Rev. B **68**, 014407 (2003).
[58] See supplementary material at http://link.aps.org/supplemental/10.1103/PhysRevB.82.075122 for space groups, magnetic structures, magnetic moments, and band gaps of materials studied.
[59] B. Hammer, L. B. Hansen, and J. K. Norskov, Phys. Rev. B **59**, 7413 (1999).
[60] H. F. Wang, Y.-I. Jang, and Y.-M. Chiang, Electrochem. Solid-State Lett. **2**, 490 (1999).
[61] A. Yamada, Y. Kudo, and K. Y. Liu, J. Electrochem. Soc. **148**, A1153 (2001).
[62] C. A. Marianetti, D. Morgan, and G. Ceder, Phys. Rev. B **63**, 224304 (2001).
[63] S. K. Mishra and G. Ceder, Phys. Rev. B **59**, 6120 (1999).
[64] O. Gunnarsson, O. K. Andersen, O. Jepsen, and J. Zaanen, Phys. Rev. B **39**, 1708 (1989).
[65] V. I. Anisimov and O. Gunnarsson, Phys. Rev. B **43**, 7570 (1991).
[66] M. Cococcioni and S. de Gironcoli, Phys. Rev. B **71**, 035105 (2005).
[67] F. Aryasetiawan, K. Karlsson, O. Jepsen, and U. Schönberger, Phys. Rev. B **74**, 125106 (2006).
[68] K. Momma and F. Izumi, J. Appl. Crystallogr. **41**, 653 (2008).
[69] C. Marianetti, G. Kotliar, and G. Ceder, Nature Mater. **3**, 627 (2004).
[70] P. Kuiper, G. Kruizinga, J. Ghijsen, G. A. Sawatzky, and H. Verweij, Phys. Rev. Lett. **62**, 221 (1989).
[71] J. van Elp, H. Eskes, P. Kuiper, and G. A. Sawatzky, Phys. Rev. B **45**, 1612 (1992).
[72] W. C. Mackrodt, N. M. Harrison, V. R. Saunders, N. L. Allan, and M. D. Towler, Chem. Phys. Lett. **250**, 66 (1996).
[73] J. Heyd and G. E. Scuseria, J. Chem. Phys. **121**, 1187 (2004).